4-3-1985

Linear Stability of a Viscous-Inviscid Interface

J. M. Hogan
General Electric Compnay

Portonovo S. Ayyaswamy
University of Pennsylvania, ayya@seas.upenn.edu

Linear Stability of a Viscous-Inviscid Interface

Abstract
In this paper the stability of the interface separating fluids of widely differing viscosities has been examined. It is shown that a viscous-inviscid (V-I) model offers a consistent zeroth-order approximation to the stability problem. The zeroth-order solution is obtained by neglecting the smallest-order effect, viz., viscosity on the less viscous side of the interface. In this sense, the V-I model significantly differs from the Kelvin-Helmholtz (K-H) approach where both the viscosities are dropped in a single step. A closed form solution for the stability criterion governing the V-I model has been obtained, and a novel instability mechanism is described. It is shown that the V-I model is also a consistent zeroth-order approximation for the Rayleigh-Taylor problem of a viscous-viscous, nonflowing interface when the viscosity ratio tends to zero. For the interface separating two viscous, nonflowing, incompressible fluids, exact solutions for the velocities, pressures, and interface displacement for a disturbance of a given wavelength have been provided for the stable (lighter fluid on top) wave motion. By discussing the roles played by the dynamic and kinematic viscosities, it is made clear why neither the V-I nor the K-H model should apply to the air-water interface. The results of the V-I model compare well with experimental observations. The V-I model serves as an excellent basis for comparison in detailed numerical studies of the viscous-viscous interface.

Disciplines
Engineering | Mechanical Engineering

Comments
Suggested Citation:
Hogan, J.M. and Portonovo S. Ayyaswamy. (1985) *Linear stability of a viscous-inviscid interface.* Physics of Fluids. Vol. 28(9).

Linear stability of a viscous–inviscid interface

J. M. Hogan
General Electric Company, Valley Forge, Pennsylvania 19101

P. S. Ayyaswamy
University of Pennsylvania, Philadelphia, Pennsylvania 19104

(Received 1 October 1984; accepted 3 April 1985)

In this paper the stability of the interface separating fluids of widely differing viscosities has been examined. It is shown that a viscous–inviscid (V–I) model offers a consistent zeroth-order approximation to the stability problem. The zeroth-order solution is obtained by neglecting the smallest-order effect, viz., viscosity on the less viscous side of the interface. In this sense, the V–I model significantly differs from the Kelvin–Helmholtz (K–H) approach where both the viscosities are dropped in a single step. A closed form solution for the stability criterion governing the V–I model has been obtained, and a novel instability mechanism is described. It is shown that the V–I model is also a consistent zeroth-order approximation for the Rayleigh–Taylor problem of a viscous–viscous, nonflowing interface when the viscosity ratio tends to zero. For the interface separating two viscous, nonflowing, incompressible fluids, exact solutions for the velocities, pressures, and interface displacement for a disturbance of a given wavelength have been provided for the stable (lighter fluid on top) wave motion. By discussing the roles played by the dynamic and kinematic viscosities, it is made clear why neither the V–I nor the K–H model should apply to the air–water interface. The results of the V–I model compare well with experimental observations. The V–I model serves as an excellent basis for comparison in detailed numerical studies of the viscous–viscous interface.

I. INTRODUCTION

In this paper we examine the linear stability of the interface between a viscous and an inviscid fluid. The fluids may be flowing or nonflowing relative to each other. The determination of the growth rates and wave propagation speeds is reduced to solving simultaneous algebraic equations. The velocities, pressures, and interfacial motions have been directly determined and closed form solutions have been found for the linear stability limit. The study of the viscous–inviscid (V–I) model of this paper has been motivated by the observation that large changes in viscosity across interfaces often arise in problems of practical interest. A consistent zeroth-order treatment of such a problem is to neglect the viscosity of the lesser viscous fluid rather than to completely eliminate both the viscosities in a single step as is done in the classical Kelvin–Helmholtz (K–H) theory. We consider the roles played by both the kinematic and dynamic viscosities in the zeroth-order limit, and provide a discussion of the physical meaning of the solution in this limit.

The developments in this study have been checked for correctness in various limiting cases. The nonflowing viscous–inviscid solution is compared with the classical Rayleigh–Taylor viscous–viscous solution in the limit of the viscosity of one of the fluids becoming vanishingly small. In the process, we also provide detailed information about actual fluid velocities that occur in the stable (lighter fluid on top) wave motion of superposed, viscous fluids. It is shown that our model provides an adequate physical description of the fluid forces acting on the interface and correctly predicts the pressure distributions in nonflowing fluids of widely differing viscosities.

The results predicted by the V–I model also compare well with the experimental results for the flow of air over oil and syrup. We discuss the predictions of the V–I model for the flowing case in light of the likely behavior of the boundary layer on the less viscous side of the interface. It is demonstrated that free stream effects can generate pressure phase shifts at the interface in instances where viscosities differ widely across the interface. In the limit of zero viscosities, results for flowing fluids coincide with those of classical Kelvin–Helmholtz theory.

The next section provides the mathematical details. For the sake of convenience we start with a general formulation of the linearized interfacial stability problem, and subsequently consider the further developments as subsets.

II. GOVERNING EQUATIONS

In this section we present the linearized equations for the perturbed motion of two superposed, incompressible fluids. The pressures and velocities are decomposed into mean and fluctuating parts and are substituted into the continuity and Navier–Stokes equations. With linearization, these equations become (with the usual notation)

$$\tilde{u}_x + \tilde{v}_y = 0\,, \tag{1}$$

$$\tilde{u}_t + U\tilde{u}_x + U_y\,\tilde{v} + \tilde{p}_x/\rho = \nu(\tilde{u}_{xx} + \tilde{u}_{yy})\,, \tag{2}$$

$$\tilde{v}_t + U\tilde{v}_x + \tilde{p}_y/\rho = \nu(\tilde{v}_{xx} + \tilde{v}_{yy})\,, \tag{3}$$

where $\tilde{u}$, $\tilde{v}$, and $\tilde{p}$ are the fluctuating components of horizontal velocity, vertical velocity, and pressure, respectively, and U is the mean component of horizontal velocity (the mean vertical component taken as zero). Subscripts in Eqs. (1)–(3) denote differentiation with respect to the appropriate variables. Next, the fluctuations are written in the form:

 0031-9171/85/092709-07$01.90

$$(\tilde{u}, \tilde{v}, \tilde{p}) \equiv (\hat{u}(y), \hat{v}(y), \hat{p}(y))\, e^{i\alpha(x-ct)}, \tag{4}$$

where α is the wavenumber and c is the complex speed. The system of equations (1)–(3) may be specialized to the two-fluid problem in which an interface separates two immiscible fluids flowing horizontally at different mean velocities. Subscripts 1 and 2 will be used to denote the upper and lower fluids, respectively. From Eqs. (1)–(3), the equations for the upper and lower fluids become

$$i\alpha\hat{u}_1 + \hat{v}_1' = 0, \tag{5}$$

$$i\alpha(U_1 - c)\hat{u}_1 + U_1'\,\hat{v}_1 + i\alpha\hat{p}_1/\rho_1 = \nu_1(\hat{u}_1'' - \alpha^2\,\hat{u}_1), \tag{6}$$

$$i\alpha(U_1 - c)\,\hat{v}_1 + \hat{p}_1'/\rho_1 = \nu_1(\hat{v}_1'' - \alpha^2\,\hat{v}_1), \tag{7}$$

with similar equations for $\hat{u}_2$ and $\hat{v}_2$. Here the primes indicate differentiation with respect to y. The kinematic and viscous boundary conditions at the interface will be addressed next. The linearized kinematic relationships between the vertical velocity and the displacement of the interface evaluated at $y = 0$ are

$$\tilde{v}_1 = \frac{\partial\eta}{\partial t} + U_1\frac{\partial\eta}{\partial x}, \tag{8}$$

with a similar expression of $\tilde{v}_2$, where η is the displacement of the interface and may be written

$$\eta = ae^{i\alpha(x-ct)}. \tag{9}$$

In terms of complex notation, the equations for $\tilde{v}_1$ and $\tilde{v}_2$ become

$$\tilde{v}_1(0) = i\alpha a(U_1 - c), \tag{10}$$

with a similar expression for $\tilde{v}_2(0)$. The continuity of shear stress at the interface is given by

$$\mu_1\left(\frac{\partial(U_1(y) + \tilde{u}_1)}{\partial y} + \frac{\partial\tilde{v}_1}{\partial x}\right) = \mu_2\left(\frac{\partial(U_2(y) + \tilde{u}_2)}{\partial y} + \frac{\partial\tilde{v}_2}{\partial x}\right), \tag{11}$$

which in complex notation becomes

$$\rho_1\nu_1\,[U_1' + \hat{u}_1' + i\alpha\hat{v}_1]_{y=0} = \rho_2\nu_2\,[U_2' + \hat{u}_2' + i\alpha\hat{v}_2]_{y=0}. \tag{12}$$

The no-slip conditions at the interface are written directly in complex notation as

$$U_1(0) = U_2(0), \quad \hat{u}_1(0) = \hat{u}_2(0). \tag{13}$$

The pressure boundary condition at the interface is

$$\sigma_{yy_2} - \sigma_{yy_1} = -T\left.\frac{\partial^2\eta}{\partial x^2}\right|_{y=0}, \tag{14}$$

where σ is the stress tensor and T is the surface tension. In terms of complex notation, Eq. (14) becomes

$$\hat{p}_1 - \rho_1 ga = \hat{p}_2 - \rho_2 ga - \alpha^2 Ta + 2\nu_1\rho_1\,\hat{v}_1' - 2\nu_2\rho_2\,\hat{v}_2'\,|_{y=0}. \tag{15}$$

III. ANALYSIS OF VISCOUS–INVISCID INTERFACE

In this section, the analysis of the viscous–inviscid interface is presented. For the flowing case, the stability threshold is determined, and the physical mechanism responsible for the instability is discussed. For the nonflowing case, the results are compared to the classical Rayleigh–Taylor solution in the limit of $\nu_2 \to 0$.

In the following, fluid 1 will be considered viscous, while fluid 2 is inviscid (Fig. 1). The gravity vector **g**, considered positive downward, can be positive or negative to allow the viscous fluid to be either above or below the inviscid fluid. The linearized perturbation equations are given by Eqs. (5)–(7), with similar equations for fluid 2, noting that $\nu_2 = 0$. The mean flow is given by a step funtion in velocity since fluid 2 is inviscid and can impose no tangential stress at its interface with fluid 1. Thus U_1' is zero in Eq. (6) and so will be U_2'. The boundary conditions given in Eq. (13) do not apply, while the shear stress condition [Eq. (12)] reduces to zero shear stress on the viscous side of the interface. This last statement is true only for the situation when ν_2 and μ_2 both equal zero. Thus, we would not expect this model to approximate the air–water interface. Note that this boundary condition differentiates the roles of the dynamic and kinematic viscosities. When $\nu_1, \mu_1 \gg \nu_2, \mu_2$, the viscous–inviscid approach eliminates small viscous effects in both the momentum equation and shear stress boundary condition. If, however, $\nu_1 \gg \nu_2$ and $\mu_1 \ll \mu_2$, as in the air–water interface, the situation is more complex. In this case we expect the boundary layer thickness to be larger on the air side as will be demonstrated subsequently. However, the fluid more accurately modeled with the zero-shear stress condition is the water. Thus the mathematical viscous–inviscid model can be a zeroth-order solution only for those interfaces for which the kinematic and dynamic viscosities are substantially larger on the one side of the interface.

A pressure equation for each fluid may be obtained by differentiating Eq. (2) with respect to x and Eq. (3) with respect to y, adding and using continuity. The end result in complex notation for fluid 1 is

$$\hat{p}_1'' - \alpha^2\hat{p}_1 = 0 \tag{16}$$

with a similar equation for $\hat{p}_2''$. The solutions for the pressures in the upper and lower fluid are

$$\hat{p}_1 = Ae^{-\alpha y} \text{ and } \hat{p}_2 = Be^{\alpha y}. \tag{17}$$

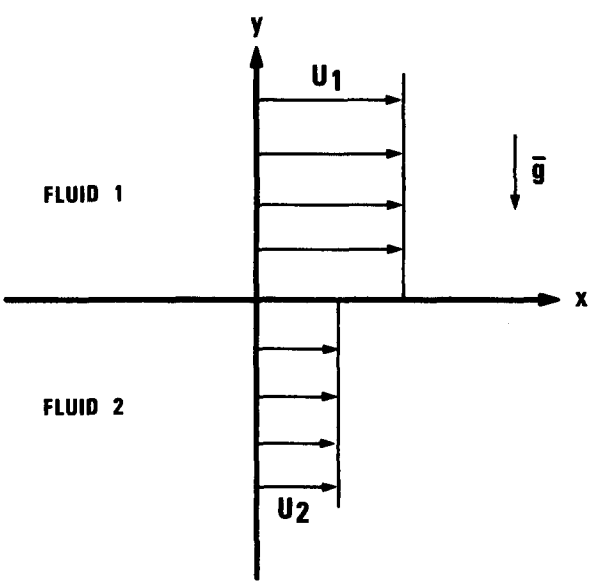

FIG. 1. Schematic of interface stability problem.

With these expressions, from Eqs. (5)–(7),

$$\hat{u}_1 = De^{-\alpha\beta y} - [A/\rho_1(U_1 - c)]\, e^{-\alpha y}, \tag{18}$$

$$\hat{v}_1 = -[iA/\rho_1(U_1 - c)]\, e^{-\alpha y} + (i/\beta)\, De^{-\alpha\beta y}, \tag{19}$$

and

$$\beta = [1 + i(U_1 - c)/\nu_1\alpha]^{1/2}. \tag{20}$$

Also, from equations for $\hat{u}_2$ and $\hat{v}_2$, setting $\nu_2 = 0$,

$$\hat{u}_2 = -Be^{\alpha y}/\rho_2(U_2 - c) \tag{21}$$

and

$$\hat{v}_2 = iBe^{\alpha y}/p_2(U_2 - c). \tag{22}$$

It is evident from Eqs. (17)–(22) that the velocities and pressures depend on the three coefficients A, B, and D. Three boundary conditions at the interface are available to explicitly determine these coefficients [Eqs. (8) (one for $\hat{v}_2$) and (9)]. The solutions for the coefficients are

$$\begin{aligned} A &= -\rho_1\alpha a(U_1 - c)^2\,[(\beta^2 + 1)/(\beta^2 - 1)], \\ B &= \rho_2\alpha a(U_2 - c)^2, \\ D &= 2\alpha a(U_1 - c)\,[\beta/(1 - \beta^2)]. \end{aligned} \tag{23}$$

The wave speed is determined by applying the pressure boundary condition at the interface. Consider Eq. (15) which is

$$\hat{p}_1 - \rho_1 ga = \hat{p}_2 - \rho_2 ga - \alpha^2 Ta - 2\nu_1\rho_1\,[\alpha^3 a\nu_1(\beta - 1)^2]. \tag{24}$$

Substituting for the pressures, this becomes

$$\begin{aligned} &\rho_2(U_2 - c)^2 + \rho_1(U_1 - c)^2 - 2i\nu_1\alpha\rho_1(U_1 - c) \\ &\quad = (g/\alpha)(\rho_2 - \rho_1) + \alpha T + 2\nu_1^2\rho_1\alpha^2(\beta - 1)^2 \end{aligned} \tag{25}$$

and is the governing equation for c. This equation represents a pair of simultaneous equations in the two unknowns c_r and c_i ($c = c_r + ic_i$). If c_i is positive, the flow is unstable with exponential growth. For c_i less than zero, disturbances decay exponentially. With $c_i = 0$, for neutral stability, we have

$$(U_1 - c_r) = -\nu_1\alpha\rho_1\,\mathrm{Im}\,[(\beta - 1)^2] \tag{26}$$

and

$$\begin{aligned} &\rho_2(U_2 - c_r)^2 + \rho_1(U_1 - c_r)^2 \\ &\quad = (g/\alpha)(\rho_2 - \rho_1) + \alpha T + 2\nu_1\rho_1\alpha^2\,\mathrm{Re}\,[(\beta - 1)^2]. \end{aligned} \tag{27}$$

Here Im and Re indicate the imaginary and real parts, respectively. Equation (26) implies that

$$U_1 = c_r \tag{28}$$

at neutral stability. From Eq. (27), with Eq. (28)

$$\begin{aligned} U_2 - U_1 &= \{(1/\rho_2)\,[(g/\alpha)(\rho_2 - \rho_1) + \alpha T]\}^{1/2} \\ &= \Delta U_{v-i}. \end{aligned} \tag{29}$$

The flow is unstable for velocity differences greater than that given by Eq. (29). Equation (29) gives the critical velocity difference as a function of the wavenumber α. With zero surface tension, there is always some α for which the critical velocity difference is below the applied velocity difference and, therefore, for which instability results. When surface tension acts, the right hand side of Eq. (29) has a minimum with respect to α. This minimum critical velocity difference defines the stability threshold for the interface. The critical wavenumber which minimizes Eq. (29) is

$$\alpha_{\mathrm{crit}} = [g(\rho_2 - \rho_1)/T]^{1/2}. \tag{30}$$

This is the solution for the linear stability of the viscous–inviscid interface.

We now discuss whether this solution is a consistent zeroth-order solution for real interfaces across which large changes in viscosity occur. Obviously, several physical mechanisms have been neglected by the viscous–inviscid approach. The transition layer between two uniform streams, for example, is characterized by two boundary layers which must develop either in time or in X. However, the mean flows in the viscous–inviscid problem are step functions independent of time and X. We now determine the conditions under which the real effects of developing boundary layers are small relative to the interaction of the outer viscous and slightly viscous streams. Consider a diffusing sheet vortex (with large viscosity ratio across the interface) as the base flow to be perturbed. The penetration of the boundary layer velocity variation into the region of uniform flow after time t is of order $(\nu t)^{1/2}$ and is more pronounced on the more viscous side of the interface (fluid 1). The distance traveled by the perturbation after time t is $C_r t$. At the linear stability threshold, in a coordinate frame moving at the average velocity of the two outer steams,

$$C_r = \Delta U/2. \tag{31}$$

Then the distance traveled by the perturbation is of order ΔUt. The times required for the vorticity to diffuse a distance equal to the length scale of the perturbation (inverse wavenumber) and for the perturbation to travel this same distance are, respectively,

$$1/\alpha^2\nu \quad \text{and} \quad 1/\Delta U\alpha. \tag{32}$$

The requirement that the time scale of the perturbation be much shorter than that of vorticity diffusion in the mean flow is then

$$\Delta U/\nu\alpha \gg 1; \tag{33}$$

i.e., the Reynolds number of the more viscous flow must be large. At the linear stability threshold, Eqs. (29) and (30) can be used to generate this requirement as

$$\left(\frac{2T^{3/2}}{\nu_1^2\,\rho_2\sqrt{g(\rho_2 - \rho_1)}}\right)^{1/2} \gg 1. \tag{34}$$

Note that the Reynolds number of the fluid on the less viscous side of the interface will now be larger yet, thus ensuring that it is consistent to retain momentum terms while neglecting viscous terms on this side of the interface.

Since the base flow is slowly varying in time, boundary layer thicknesses can eventually become large even for large Reynolds numbers based on the wavenumber. Therefore, an independent restriction must be placed on the boundary layer thickness, namely,

$$\delta\alpha \ll 1,$$

to ensure that the deviation from uniform flow is restricted to a region which is small compared to the disturbance wavelength. With these restrictions, the velocities and pressures for either of the two viscous fluids (with widely different

viscosities) flowing relative to each other can be written as

$$U = U^{(0)} + \epsilon U^{(1)}, \quad \hat{u} = \hat{u}^{(0)} + \epsilon \hat{u}^{(1)},$$
$$\hat{v} = \hat{v}^{(0)} + \epsilon \hat{v}^{(1)}, \quad \hat{p} = \hat{p}^{(0)} + \epsilon \hat{p}^{(1)},$$

where ϵ is the ratio of viscosities ν_2/ν_1. Here $U_1^{(0)}$ and $U_2^{(0)}$ form a step function across the transition region, and effects dependent on the viscosity ratio are contained in terms multiplied by ϵ. Substituting these expressions in Eqs. (5)–(7), using the appropriate boundary conditions, and collecting terms of zeroth order, results in the viscous–inviscid formulation presented in our paper. For the quiescent (nonflowing) case, this zeroth-order consistency is further demonstrated by letting ϵ tend to zero in the actual solution that is valid for two viscous fluids. As will be shown subsequently, the solution under this limit matches the viscous–inviscid result.

The mechanism of the viscous–inviscid instability is best understood in terms of work done by pressure forces of the viscous fluid on the interface between the viscous and inviscid fluids. Evaluated at $y = 0$, the location of interface, this pressure is

$$\tilde{p} = -\rho_1 \alpha (U_1 - c)^2 \left[(\beta^2 + 1)/(\beta^2 - 1)\right] \eta . \tag{35}$$

With β given by Eq. (20), this becomes

$$\tilde{p} = \rho_1 \alpha^2 \nu_1 (U_1 - c) i\eta - \rho_1 \alpha (U_1 - c)^2 \eta . \tag{36}$$

The first term in the above is caused by viscosity. It is the second inviscid term which describes the increase in pressure at the wave troughs and the decrease in pressure at the wave crests. This basic pressure field results from the change in flow area experienced by the upper stream as it flows over the waveform. The second term in Eq. (36) is quadratic and for real values of the wave speed, c, is in antiphase with η irrespective of the sign of $(U_1 - c)$. The phasing of the viscous term relative to the basic pressure field depends on the sign of $(U_1 - c)$. However, inspection of this equation shows that the phase shift of the pressure component caused by viscosity is always in the direction of the velocity of the viscous fluid relative to the waveform. This effect is shown in Fig. 2. In the upper diagram, the viscous flow to the right is relative to the waveform and points such as B experience a decrease in pressure, while points such as D experience an increase. The basic pressure field has a decrease at points like A and an increase at points like C. The viscous component of pressure is thus shifted to the right of the basic pressure field, in the direction of the viscous flow relative to the waveform. In the lower diagram, the viscous component of the pressure relative to the basic pressure fields is shifted to the left, again in the direction of the viscous flow relative to the waveform.

The rate of sinking of the interface, $-\partial\eta/\partial t$, is given by

$$-\frac{\partial \eta}{\partial t} = i\alpha c \eta . \tag{37}$$

Comparison of the last two equations shows the pressure perturbation caused by viscosity [first term in Eq. (36)] to be in phase with the rate of sinking of the interface for U_1 greater than c (viscous fluid overtaking wave) and 180° out of phase with the rate of sinking of the interface for U_1 less than c (wave overtaking viscous fluid—see Fig. 2). In the former case, the integral of $p_1(-\partial\eta/\partial t)$ over each wavelength is positive and, therefore, net work is done on the interface

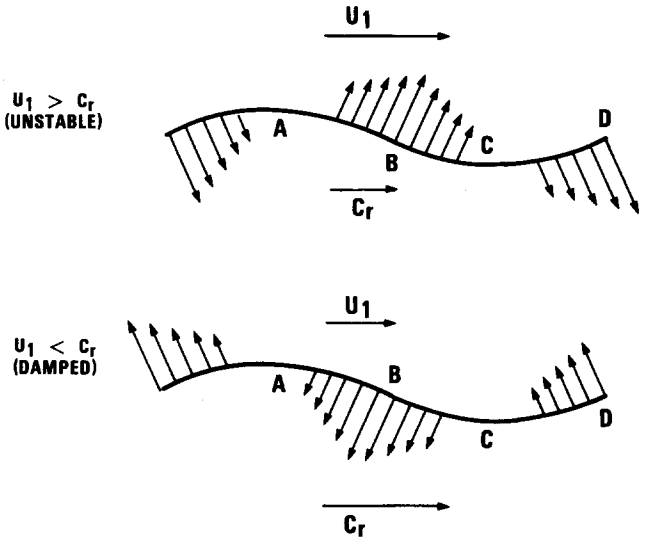

FIG. 2. Phasing of pressure with respect to interface. Arrows indicate pressure component caused by viscosity (positive where arrows are downward).

feeding energy into the growth of the instability. Physically, the component of pressure caused by viscosity increases where the interface sinks away from the viscous fluid and decreases where the interface rises into the viscous fluid, in each case enhancing the growth of the disturbance. When the pressure is 180° out of phase with the rate of sinking, damping of interface motion occurs by a similar argument, i.e., now the pressure component caused by viscosity increases where the interface attempts to rise into the viscous fluid and decreases where the interface attempts to sink away from the viscous fluid. Thus, only for $c_r = U_1$ can neutral stability occur [as previously shown in Eq. (28)]. The effect of viscosity is then to change the phasing of the pressure perturbation with respect to the interface, thus allowing work to be done on the interface by the two uniform flows. Previous physical arguments given by Jeffreys,[1] Miles,[2,3] Brooke Benjamin,[4,5] Lighthill,[6] and Mollo-Christensen[7] in explaining the mechanism of water wave generation by sheared airflows depend on boundary layer phenomena for the pressure phase shift. The present analysis, however, shows that the simple free stream flow of a viscous fluid over the disturbance waveform generates pressure perturbations capable of performing work on the interface.

A. Rayleigh–Taylor flow

We now consider the case of zero mean flow with a full accounting of viscosity on both sides of the interface. This classical problem has been studied by a large number of investigators and the monographs by Chandrasekhar,[8] Yih,[9] Drazin and Reid[10] provide the historical, theoretical, and experimental developments in this regard. The articles by Axford,[11] Menikoff, Mjolsness, Sharp and Zemach,[12] Menikoff, Mjolsness, Sharp, Zemach, and Doyle,[13] Bernstein and Book,[14] and Baker[15] also contain important information related to this problem and review earlier papers. We shall rederive the dispersion equation in a slightly different form from those of the previous investigators. The limits of the

dispersion equation for the viscosity ratio tending to zero will be examined, and the pressure difference across the interface under this limit determined. We then compare these results to the viscous–inviscid formulation discussed earlier.

First, we set $U_1 = U_2 = U_1' = U_2' = 0$ in the governing equations and solve the resulting system to obtain

$$\begin{aligned}
&\hat{u}_1 = \overline{D} e^{-\alpha\beta_1 y} + \overline{A} e^{-\alpha y}, \\
&\hat{v}_1 = i\overline{A}/\rho_1 c + (i\overline{D}/\beta_1)\, e^{-\alpha\beta_1 y}, \\
&\hat{u}_2 = \overline{E} e^{\alpha\beta_2 y} + \overline{B} e^{\alpha y}, \\
&\hat{v}_2 = -(i\overline{E}/\beta_2)\, e^{\alpha\beta_2 y} - (i\overline{B}/\rho_2 c)\, e^{\alpha y}, \\
&\beta_1 = (1 - ic/\nu_1\alpha)^{1/2}, \quad \beta_2 = (1 - ic/\nu_2\alpha)^{1/2}.
\end{aligned} \tag{38}$$

The four boundary conditions given by Eq. (10) and a similar one for $\hat{v}_2(0)$, (12), and (13) may be used to solve for $\overline{A}$, $\overline{B}$, $\overline{D}$, and $\overline{E}$. These constants are then substituted into Eq. (38) to obtain the velocities as a function of the wave speed c. The wave speed itself is determined from the pressure boundary condition at the interface. This may be written as

$$\begin{aligned}
\overline{A} - \rho_1 g a = \overline{B} - \rho_2 g a - \alpha^2 T a + 2\nu_1\rho_1 \\
\times [-i\alpha\overline{A}/\rho_1 c - i\alpha\overline{D}] - 2\nu_2\rho_2 \\
\times [-i\alpha\overline{B}/\rho_2 c - i\alpha\overline{E}].
\end{aligned} \tag{39}$$

This equation is nondimensionalized by division throughout with $(\sqrt{g\alpha}\, a)$. Additionally, we introduce $c_N = c\sqrt{\alpha/g}$, $\theta_1 = \nu_1\alpha^{3/2}/\sqrt{g}$, $\theta_2 = \nu_2\alpha^{3/2}/\sqrt{g}$, and $J = \rho_1/(\rho_2 - \rho_1)$. Here c_N is the nondimensional complex wave speed. Letting $c_N = c_{rN} + ic_{iN}$, the pressure boundary condition becomes

$$\begin{aligned}
B_N c_N(\rho_2/\rho_1) J - A_N c_N J = 1 + \alpha^2 T/g(\rho_2 - \rho_1) \\
+ 2Ji\theta_1(A_N + D_N) - 2J(\rho_2/\rho_1) i\theta_2(B_N + E_N),
\end{aligned} \tag{40}$$

where

$$\begin{aligned}
&A_N = [(\beta_2 - 1)/(\beta_1 - 1)]\,\{F_N\} - 2c_N/(\beta_1 - 1) - c_N, \\
&B_N = F_N + c_N, \\
&D_N = -[(\beta_2 - 1)/(\beta_1 - 1)]\,\{F_N\} + \frac{2c_N\beta_1}{(\beta_1 - 1)}, \\
&E_N = -\beta_2 F_N.
\end{aligned} \tag{41}$$

In Eq. (41) we have introduced

$$\begin{aligned}
&\beta_1 = (1 - ic_N\sqrt{g}/\nu_1\alpha^{3/2})^{1/2}, \\
&\beta_2 = (1 - ic_N\sqrt{g}/\nu_2\alpha^{3/2})^{1/2},
\end{aligned}$$

and

$$F_N = \frac{2[c_N + (m-1)i(\nu_1\alpha^{3/2}/\sqrt{g})(\beta_1 - 1)]}{(\beta_1 - 1)(\rho_2/\rho_1) + (\beta_2 - 1)}.$$

We note that c_N is completely specified by the four nondimensional parameters ρ_2/ρ_1, $\alpha^2 T/g(\rho_2 - \rho_1)$, θ_2, and ν_2/ν_1. Equation (40) actually represents two equations, one real and one imaginary which can be solved simultaneously for the real and imaginary wave speeds c_r and c_i. The solution of these equations is straightforward using standard numerical routines. Once c_r and c_i are known, the constants $\overline{A}$, $\overline{B}$, $\overline{D}$, and $\overline{E}$ may be evaluated. The fluid velocities and pressures are then known functions of η, y, and t for a wave of initial height a and wavenumber α.

For zero surface tension, our equation (40) is identical to Eq. (33) of Ref. 9 (see Chap. 4, Sec. 3), derived earlier by Chandrasekhar.[8] The present form for the dispersion equation is favored because the constants $\overline{A}$, $\overline{B}$, $\overline{D}$, and $\overline{E}$ also appear in the expressions for the velocities. Thus, once they are numerically evaluated, the wave velocity as well as the fluid velocities are known.

The actual fluid velocities that occur in the stable wave motion of superposed viscous fluids do not seem to have appeared in published literature and are included here for completeness. If the velocities are nondimensionalized in the same way as the wave speed c (with $\sqrt{g/\alpha}$), they will still depend on the initial wave height a. It proves more convenient, therefore, to define $u_N = u/\sqrt{g\alpha}\, a$. Then the x components of velocity are given by

$$\begin{aligned}
&\hat{u}_{1N}(y) = D_N e^{-\beta_1\alpha y} + A_N e^{-\alpha y}, \\
&\hat{u}_{2N}(y) = E_N e^{\beta_2\alpha y} + B_N e^{\alpha y}.
\end{aligned} \tag{42}$$

These velocities are plotted for the typical cases of air–water and air–oil interfaces in Figs. 3 and 4, respectively. Profiles have been shown over one complete period. Of particular interest is the fact that the fluid in the boundary layers is leading the inviscid far-field solution. Such a phenomenon occurs in other oscillating flow situations. For example, in oscillating pipe flow, or oscillating boundary layers adjacent to flat plates, the flow adjacent to the wall reverses before the outer flow does. In these flows, as well as in the current study, the pressure gradient (dp/dx) acting on the flow with-

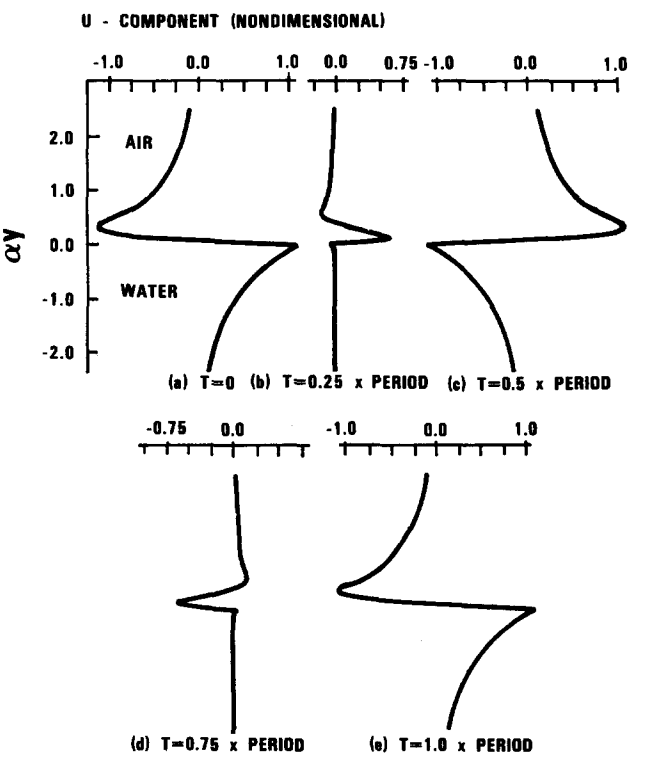

FIG. 3. Velocity profiles on air–water interface. Wavelength = 0.03 m, $\theta_2 = 9.3\times10^{-4}$, $\nu_2/\nu_1 = 0.066$, $\rho_2/\rho_1 = 820$, $\alpha^2 T/g(\rho_2 - \rho_1) = 0.316$, $c_{rN} = 1.1455$, $c_{iN} = 0.202\times10^{-2}$.

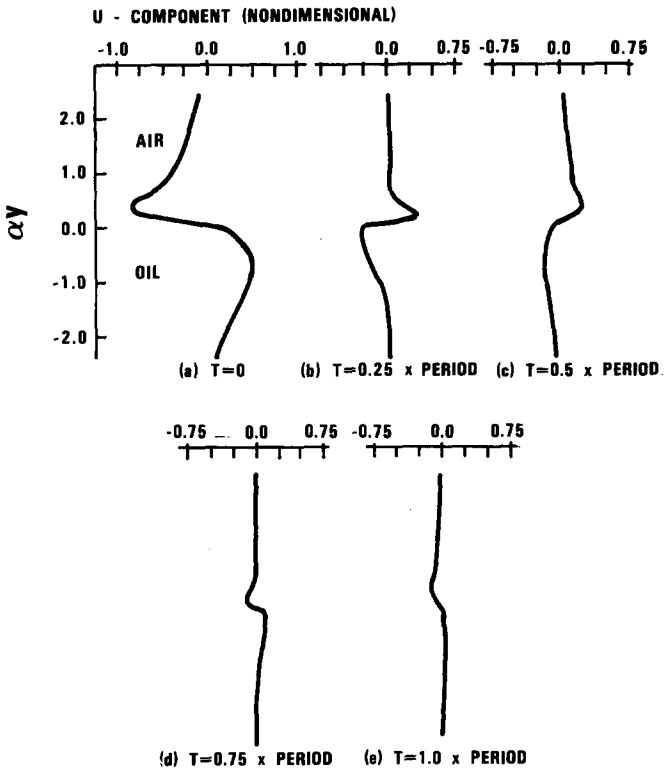

FIG. 4. Velocity profiles on air–oil interface. Wavelength = 0.03 m, $\theta_2 = 0.263$, $\nu_2/\nu_1 = 18.75$, $\rho_2/\rho_1 = 738$, $\alpha^2 T/g(\rho_2 - \rho_1) = 0.144$, $c_{rN} = 0.911$, $c_{iN} = 0.319$.

in the boundary layer is essentially the same as the pressure gradient acting on the flow outside the boundary layer. However, the fluid within the boundary layer has lower momentum and, therefore, responds more rapidly to the changing pressure gradient.

The limit of the dispersion equation as $\nu_2 \to 0$ while ρ_2/ρ_1 remains finite is investigated next. This case simulates the interface between oil and water. In this situation $\beta_2 \to \infty$ and $m \to 0$. The dispersion equation becomes

$$c_N{}^2(\rho_1 + \rho_2) + 4i\theta_1\rho_1 c_N = (\rho_2 - \rho_1) + \alpha^2 T/g + 4\rho_1\theta_1{}^2\,[1 - (1 - ic_N/\theta_1)^{1/2}]\,. \tag{43}$$

For $\theta_1 \ll 1$ this equation simplifies to

$$c_N^2\,(\rho_1 + \rho_2) + 4\theta_1\rho_1 c_N i - (\rho_2 - \rho_1) - \alpha^2 T/g = 0\,, \tag{44}$$

the solution of which is

$$c_{Nr} = \{c_{No}^2 - [2\theta_1\rho_1/(\rho_1 + \rho_2)]^2\}^{1/2} \tag{45}$$

and

$$c_{Ni} = -2\theta_1\rho_1/(\rho_1 + \rho_2)\,, \tag{46}$$

where c_{No} is the inviscid wave speed.

The pressure difference across the interface plays a crucial role in the damping of stable interfacial motion. By nondimensionalizing this pressure difference with $\Delta\rho g/\alpha$, we have

$$\Delta p_N = \frac{\rho_2 c_N \alpha B_N}{\Delta\rho}\,\eta - \frac{\rho_1 c_N \alpha A_N}{\Delta\rho}\,\eta + \frac{\alpha(\rho_1 - \rho_2)}{\Delta\rho}\,\eta\,. \tag{47}$$

In the limit of $\nu_2 \to 0$ this pressure difference becomes

$$\lim_{\nu_2 \to 0} \Delta p_N = [a\,c_N^2\,(\rho_1 + \rho_2)/\Delta\rho]\,\eta + (\alpha/\Delta\rho)\,(\rho_1 - \rho_2)\,\eta + (2\rho_1/\Delta\rho)\,c_N\,\alpha i\theta_1\eta\,. \tag{48}$$

The first two terms of this equation form the inviscid result for the pressure difference. The last term contains the viscous effects and only depends on the viscous properties of fluid 1. Note that in this development the no-slip interface condition has not been violated under this limit. The kinematic viscosity ν_2 is arbitrarily small but still nonzero. The boundary layer in fluid 2, however, is sufficiently small so that its effect on the interfacial pressure difference may be ignored in comparison to the viscous effects on this pressure difference resulting from the motion of fluid 1.

B. Comparisons of the Rayleigh–Taylor flow with the viscous–inviscid development

Consider Eq. (43). This is the formal limit of the viscous–viscous Rayleigh–Taylor formulation as $\nu_2 \to 0$ (the limit as the boundary layer thickness tends to zero). On the other hand, Eq. (25) was obtained by ignoring the no-slip condition and the viscosity (the boundary layer) on the less viscous side of the interface. Letting $U_1 = U_2 = 0$, and introducing c_N and θ, Eq. (25) reduces to Eq. (43). Thus, the dispersion equation for interfaces separating real fluids of sufficiently different viscosities is properly modeled by the viscous–inviscid approach. Also, it is easy to show that the pressure difference across the interface for the viscous–inviscid model is identical to Eq. (48), the formal limit of the pressure difference in the viscous–viscous formulation for $\nu_2 \to 0$.

C. Kelvin–Helmholtz problem

Here the flow of one inviscid fluid relative to another inviscid fluid is considered. The equation for the wave motion can be found by setting $\nu_1 = \nu_2 = 0$ in Eqs. (5)–(7) and the similar ones for $\hat{u}_2$, $\hat{v}_2$, and eliminating the boundary conditions given by Eqs. (12) and (13). The resulting wave equation is

$$\rho_2(U_2 - c)^2 + \rho_1(U_1 - c)^2 = (g/\alpha)\,(\rho_2 - \rho_1) + \alpha T\,. \tag{49}$$

The solution of which is

$$c = \frac{\rho_2 U_2 + \rho_1 U_1}{\rho_2 + \rho_1} \pm \left[\frac{g}{\alpha}\,\frac{(\rho_2 - \rho_1)}{(\rho_2 + \rho_1)} + \frac{\alpha T}{(\rho_2 + \rho_1)} - \rho_1\rho_2\left(\frac{U_2 - U_1}{\rho_1 + \rho_2}\right)^2\right]^{1/2}. \tag{50}$$

The flow is unstable ($c_i > 0$) for

$$\Delta U_{i-i} = U_2 - U_1 > [(\rho_1 + \rho_2)/\rho_1\rho_2]^{1/2} \times [(g/\alpha)(\rho_2 - \rho_1) + \alpha T]^{1/2}. \quad (51)$$

First we note that in the limit of $\nu_1 \to 0$, Eq. (25) reduces to the inviscid–inviscid Eq. (49). Next, note that the viscous–inviscid critical velocity difference, ΔU_{v-i} [Eq. (29)], is related to the classical inviscid–inviscid critical velocity difference, ΔU_{i-i} [Eq. (51)], as follows:

$$\Delta U_{v-i} = [\rho_1/(\rho_1 + \rho_2)]^{1/2} \Delta U_{i-i}. \quad (52)$$

Thus, the viscous–inviscid interface has a smaller stability threshold than that of the inviscid–inviscid interface. Equation (52) is identical to the result obtained by Weissman[16] for a model that included a small amount of viscosity in one layer of the Kelvin–Helmholtz flow. The present analysis, however, shows that this equation is valid for any level of viscosity on the viscous side of the viscous–inviscid interface.

IV. CONCLUSIONS

It is interesting to qualitatively compare the predictions of the viscous–inviscid theory with observations of the motions of real interfaces. Recall that for the air–water interface, the Kelvin–Helmholtz solution predicts a critical velocity difference of 6.5 m/sec, whereas Jeffries lists critical velocities for flow over ponds between 0.2 and 1.3 m/sec. For such large-scale flows, determination of the velocity directly above the water surface is difficult. Laboratory data on the air–water interface is not readily available. On the other hand, Francis[17,18] has documented experiments suggesting fair agreement between Kelvin's classical stability analysis and measured critical velocities for interfaces between air and two types of oil and air and syrup. Oil kinematic viscosities were 2.5 and 29 stokes (S) (17 and 197 times the viscosity of air, respectively). Syrup kinematic viscosity was 578 S or 3932 times the viscosity of air. Velocity profiles of the air were not uniform directly above the oil or syrup, and Francis had to resort to an extrapolated value of the air velocity at 0.05 cm above the undisturbed interface for comparison with Kelvin's critical velocity equation. This extrapolated value was in good agreement with Kelvin's theoretical velocity. Clearly, such agreement is somewhat dependent on the extrapolation height above the interface. Of more significance is the fact that Francis' critical velocities did not depend on the viscosity of the oil or syrup—varied through the experiments by a factor of 230. This result is not a function of the extrapolation height and is apparently a characteristic of interfaces separating fluids of widely differing viscosities. Our viscous–inviscid stability theory satisfactorily explains the results noted by Francis. Note that Eq. (34) is satisfied for the air–oil interface, ensuring the applicability of the viscous–inviscid solution as a consistent zeroth-order approach. Equation (52) gives the relationship between the critical velocities of the viscous–inviscid interface and the inviscid–inviscid interface. For conditions prevailing in Francis' experiments, the equation shows these velocities to be essentially equal, i.e., $\rho_2 \ll \rho_1$. Thus, agreement between Francis' viscous–inviscid experiments and Kelvin's inviscid–inviscid analysis is to be expected. In fact, for those interfaces separating liquid and gas in which the liquid can be modeled as viscous and the gas as inviscid, the two theories are in essential agreement on the value of the critical velocity. The present viscous–inviscid theory predicts no dependence of the critical velocity on the kinematic viscosity of the viscous fluid [see Eq. (29)]. This prediction is in excellent agreement with the results of Francis' experiments in which liquid viscosity was varied by a factor of 230 with no effect on the critical velocity.

The present formulation makes it clear why neither the V–I nor the K–H model is a valid approximation for the air–water interface—in neither case can an argument be made for zero-order consistency. It is important to note that the V–I model contains the classical K–H result as a proper subset. In this sense, the results are more general and useful. In this same context, previous investigations of the stability threshold[16] have been restricted to the study of interfaces between inviscid and weakly viscous fluids only. The results derived here, Eq. (52), are an exact solution for the stability threshold for any level of viscosity on the viscous side.

ACKNOWLEDGMENTS

The authors gratefully acknowledge the many helpful discussions they have had with Professor T. Sundararajan and Professor M. W. Nansteel.

One of the authors (J.M.H.) gratefully acknowledges the financial support of the General Electric Company, Valley Forge, Pennsylvania, during the course of the present investigation.

[1] J. Jeffreys, Proc. R. Soc. London **107**, 189 (1925).
[2] J. W. Miles, J. Fluid Mech. **3**, 185 (1957).
[3] J. W. Miles, J. Fluid Mech. **6**, 583 (1959).
[4] T. Brooke Benjamin, J. Fluid Mech. **6**, 161 (1959).
[5] T. Brooke Benjamin, J. Fluid Mech. **9**, 513 (1960).
[6] M. J. Lighthill, J. Fluid Mech. **14**, 385 (1962).
[7] E. L. Mollo-Christensen, *Illustrated Experiments in Fluid Mechanics* (MIT Press, Cambridge, MA, 1972), pp. 113–120.
[8] S. Chandrasekhar, *Hydrodynamic and Hydromagnetic Stability* (Clarendon, Oxford, 1961).
[9] C-S. Yih, *Stratified Flows* (Academic, New York, 1980).
[10] P. G. Drazin and W. H. Reid, *Hydrodynamic Stability* (Cambridge U. P., Cambridge, England, 1981).
[11] R. A. Axford (private communication).
[12] R. Menikoff, R. C. Mjolsness, D. H. Sharp, and C. Zemach, Phys. Fluids **20**, 2000 (1977).
[13] R. Menikoff, R. C. Mjolsness, D. H. Sharp, C. Zemach, and B. J. Doyle, Phys. Fluids **21**, 1674 (1978).
[14] I. B. Bernstein and D. L. Book, Phys. Fluids **26**, 453 (1983).
[15] L. Baker, Phys. Fluids **26**, 950 (1983).
[16] M. A. Weissman (private communication).
[17] J. R. D. Francis, Philos. Mag, Ser. 7 **45**, 695 (1954).
[18] J. R. D. Francis, Philos. Mag, Ser. 8 **1**, 685 (1956).